



New magnetic chelating sorbent for chromium speciation by magnetic solid phase extraction on-line with inductively coupled plasma optical emission spectrometry

I. Morales-Benítez¹, P. Montoro-Leal¹, J.C. García-Mesa¹, M.M. López Guerrero^{*}, E. Vereda Alonso^{**}

Department of Analytical Chemistry, Faculty of Sciences, University of Málaga, Campus de Teatinos, 29071, Málaga, Spain

ARTICLE INFO

Handling Editor: J. L. Burguera

Keywords:

Chromium speciation
Magnetic solid phase extraction
Inductively coupled plasma optical emission spectrometry
Environmental water samples

ABSTRACT

A novel sorbent material employing magnetic nanoparticles (MNPs) coupled to graphene oxide (GO) functionalized with 4-aminobenzenesulfonic acid (M@GO-ABS) has been synthesized and applied to develop an inexpensive and automatic method for Cr(III) and Cr(VI) speciation in environmental samples; the developed method combines inductively coupled plasma optical emission spectrometry (ICP-OES) with on-line magnetic solid phase extraction (MSPE). Two magnetic-knotted reactors containing M@GO-ABS were installed in the eight-port injection valve of a flow injection (FI) manifold. Two different eluents were used, one for Cr(VI) (the most toxic chromium species) and one for total Cr concentration. Cr(III) concentration was calculated by the difference between Cr(VI) concentration and total Cr concentration. The optimized method presented detection limits (LOD, peak height) of $0.1 \mu\text{g L}^{-1}$ for chromium (VI) and $0.08 \mu\text{g L}^{-1}$ for total chromium, and enrichment factors of 15 and 23, respectively. Certified reference materials (TMDA 54.5 fortified lake water and SPS-SW2 surface water) and spiked aqueous samples were used to validate the developed method. The developed method was fruitfully applied to chromium speciation in environmental water samples such as seawater, well water and tap water collected in Málaga (Spain). The obtained values were in good agreement with the certified values, and the recoveries were found in the range of 91–108% for the spiked samples.

1. Introduction

Chromium is found in small quantities associated with other metals, such as iron, in nature. Due to industry applications such as metallurgy or tannery, large quantities of chromium compounds are released into the environment [1]. As consequence, both natural and anthropogenic chromium enter into the food chain through water, soil and air, and consequently, Cr reaches the human body as a toxic and dangerous contaminant [2–4].

In the nature, the oxidation states range of chromium is from 0 to VI. The two species determined to be chemically stable are Cr(III) and Cr(VI), and therefore, both species naturally persist in the environment [5]. Chromium (III) plays an important role in metabolic processes by enhancing the activity of certain enzymes and stimulating the synthesis of cholesterol and fatty acids [6]. Chromium (III) can be found as an

ingredient in some commercially available complex compounds, medicines, medicinal products (like chromium picolinate pills, Centrum multivitamin products, Béres-drops, etc.). In the Netherlands, the estimated average daily total Cr intake is $100 \mu\text{g}$, with a range of 50–200 μg [7].

However, the anion derivative of Cr(VI), due to its toxic nature and small size that allows it to easily penetrate through biological cell membranes, is recognized as a carcinogenic and mutagenic substance. United States Environmental Protection Agency (EPA) established hexavalent chromium as a highly toxic species and as a class I human carcinogen by the International Agency for Research on Cancer (IARC). For human's health, EPA has set a limit of $100 \mu\text{g L}^{-1}$ of total chromium in drinking water.

World regulatory agencies strictly recommend maximum tolerable limits for chromium in drinking water globally. The United States

* Corresponding author.

** Corresponding author.

E-mail addresses: mmlopez@uma.es (M.M. López Guerrero), eivereda@uma.es (E. Vereda Alonso).

¹ Equally contribution.

Environmental Protection Agency indicated that the maximum concentration of total chromium allowed in drinking water is 0.1 mg L^{-1} and the World Health Organization (WHO) considered the maximum concentration admissible for Cr(VI) in drinking water as 0.05 mg L^{-1} [7–9].

Thus, the opposite physiological effect of chromium (III) and (VI) has made necessary to develop analytical methods to determine the concentration of both species in natural and processed samples (drinking water, surface water, sea water, blood serum, food products, medicinal products, etc.). The speciation study requires high-capacity separation and high sensitivity detection because chromium naturally exists in small quantities. Since some chromium species are responsible for toxicity and adverse physiological effects, the need for chromium speciation and not the total Cr concentration is of paramount importance [10,11]. In addition, the development of automated, high-speed, and uncomplicated methods is necessary, since the monitoring and control of these trace sources of Cr in the environment requires the processing of many samples to accurately characterize their abundance and reach reliable conclusions.

Generally, speciation methods are coupled techniques and can be categorized as on-line or off-line techniques. In on-line speciation the sample is directly analyzed after a previous species separation/enrichment. In off-line speciation the separation and enrichment of chemical species are isolated in time and space from the analytical technique. Thus, a sample pretreatment before instrumental analysis is a very important topic for analytical investigators. Some pretreatment methods are liquid-liquid extraction [11,12], solid-phase extraction [13,14], capillary microextraction and cloud point extraction [15,16]. But these methods are off-line, and the operation process is time-consuming and laborious. Therefore, it remains an urgent requirement to develop an automated on-line extraction and analysis system for chromium speciation. Thus, in recent years, notable efforts have been established to acquire new methodologies in sample handling methods.

Solid phase extraction (SPE) is an extensively applied methodology considered appropriate for sample pretreatment and preconcentration purposes. Recently, magnetic solid-phase extraction (MSPE) is an innovative miniaturized separation technique that requires a low amount of sample and solvents for sorption-desorption steps. As sorbents, modified or functionalized magnetic nanoparticles (MNPs) can be used, overall, for applications in the fields of trace metal ion preconcentration and separation. Superficially modified MNPs with, such as silica, alumina, carbon nanotubes (CNTs), graphene oxide (GO), polymer, surfactant, analytical reagent surfactants etc., can be used to improve the coating efficiency and stability [17–19].

In this work, a new patented magnetic graphene oxide [20] [P202030050], was functionalized with 4-aminobenzenesulfonic acid. The new material called (M@GO-ABS) has been thoroughly characterized. This material was synthesized by double chemical link, between iron oxide MNPs and GO, and between 4-aminobenzenesulfonic acid with MNPs and GO. Furthermore, due to its amino group, ABS was easily anchored to M@GO through an imide bond. The double chemical bond gives the material greater stability and durability. Additionally, the functional group added to M@GO contains S and N which facilitates the formation of complexes between the material and the metals. Using this material as sorbent, a novel on-line method for preconcentration and determination of trace amounts of Cr(III) and Cr(VI) via flow injection inductively coupled plasma optical emission spectrometry (FI-ICP-OES) has been designed and utilized for the analysis of environmental water samples.

The validation of the proposed method for the speciation of Cr(III) and Cr(VI) has been carried out by analyzing the certified reference materials, TMDA 54.5 and SPS-SW2, and by added water samples from Málaga (Spain), tap water, well water and sea water samples.

2. Experimental

2.1. Instrumentation

An inductively coupled plasma optical emission spectrometer, Optima 7300 DV (PerkinElmer, Waltham, MA, USA) and a AS-91 auto-sampler (PerkinElmer, Waltham, MA, USA) coupled with a FIAS 400 AS system (PerkinElmer, Waltham, MA, USA) were employed throughout. The FIAS manifold was directly linked to the ICP and was operated by Optima software. The operating conditions shown in Table 1 are the optimal ones. The selected analytical line was Cr 205.56 nm.

50 mg of M@GO-ABS were packaged in a PTFE tube (500 mm × 0.5 mm i. d.). The M@GO-ABS tube was wrapped around a Nd/Fe/B toroidal magnet (2 T, 81.4 N holding strength) and sandwiched between two other equal Nd/Fe/B magnets. This reactor was on an eight-port rotary valve of the FIAS 400 system. Two polyethylene frits (Omnifit, Cambridge, UK) were installed at both ends of the knotted reactor (R) to prevent material loss. PTFE pump tubings were employed to distribute the samples, chemicals, and waste. The FIAS 400 system was connected and controlled synchronously with the ICP-OES.

A Spectrum 100 FT IR spectrometer (PerkinElmer, Shelton, CT, USA) was utilized to record IR Spectra (approximately 1% (wt/wt) potassium bromide pellets).

A X-ray photoelectron spectroscopy (XPS) PHI 5700 instrument (Physical Electronics, Chanhassen, MN, USA) with a Mg K_{α} X-ray excitation source ($h\nu = 1253.6 \text{ eV}$) was used; binding energies (BE) were determined relative to the position of the C 1 s peak at 284.8 eV. The residual pressure in the analysis chamber was maintained below 3×10^{-9} Torr during data acquisition. The novel functionalized M@GO-ABS micro-structures were observed by a transmission electron microscopy (TEM) (JEOL JEM-1400, Peabody, MA, USA). N_2 adsorption isotherms (Micromeritics ASAP 2020 V4.02, Norcross, GA, USA) was used. CHNOS elemental analysis (LECO TruSpec Micro CHNSO, St. Joseph, MI, USA) was used to study the composition of the material.

2.2. Reagents and samples

High purity chemicals were utilized for all experiments. All plastic and glassware were washed with concentrated nitric acid and stored filled in nitric acid 10% (wt/wt); the materials were washed several times with water previously to be employed. Doubly de-ionized water (DDW) ($18 \text{ M}\Omega \text{ cm}$) obtained from a Milli-pore Milli-Q water system (Milli-pore, Bedford, MA, USA) was always utilized.

Synthesis of M@GO-ABS. $\text{FeCl}_3 \cdot 6\text{H}_2\text{O}$, $\text{FeCl}_2 \cdot 4\text{H}_2\text{O}$, NH_4OH 30% (wt/wt), CH_3OH , NaCl , glacial acetic acid and H_2SO_4 98% were supplied by Merck (Merck, Darmstadt, Germany) and H_2O_2 35% by Scharlab (Scharlab, Barcelona, Spain). 3-Aminopropyltriethoxysilane was acquired from Fluka (Fluka, Buchs, Switzerland). Tetraethoxysilane (TEOS), N,N-dicyclohexylcarbodiimide (DCC), glutaraldehyde,

Table 1
Optimal conditions for the FIAS-400 system.

Step	Pump	Solution	Valve	Flow rate (mL min^{-1})	Time (s)	Track
1	P1	Sample	A	1.3	180	Waste
	P2	–	A	–	180	–
2	P1	DDW	A	1.5	30	Waste
	P2	–	A	–	30	–
3	P1	Sample	B	1.3	180	Waste
	P2	NH_4OH	B	3	80	ICP-OES
4	P1	DDW	B	1.5	30	Waste
	P2	NH_4OH	B	3	30	ICP-OES
5	P1	HNO_3	A	2.5	60	Waste
	P2	HNO_3	A	4.2	60	ICP-OES

sulfanilic acid, ethylenediamine (EDA), graphite, NaNO_3 and KMnO_4 were acquired from Aldrich Chemie (Aldrich Chemie, Steinheim, Germany) and ethanol (Carlo Erba, Milano, Italy) were used for the synthesis and functionalization of M@GO-ABS.

Hydrochloric and nitric acid, and glycine (Merck, Darmstadt, Germany) were used as eluent and buffer preparation reagents. Standards 1000 mg L^{-1} for Cr(III) solution and $\text{K}_2\text{Cr}_2\text{O}_7$ 99.99% for Cr(VI) (Merck, Darmstadt, Germany) were employed. Prior to use, the working standards were prepared by appropriate dilution.

The pH 3 buffer was obtained by mixing 11.4 mL hydrochloric acid 0.2 M with 50.0 mL of glycine 0.2 M and leveling with DDW to 100 mL.

3.2% (wt/wt) NH_4OH (Merck, Darmstadt, Germany) was utilized as a selective eluent for Cr(VI) elution and determination; and 2.3% (wt/wt) HNO_3 was used as eluent for total Cr elution.

2.3. Sample preparation

The certified reference materials (CRMs), TMDA 54.4 fortified lake water and SPS-SW2 132 Reference Material for Measurement of Elements in Surface Waters, were studied to determine the accuracy of the

developed method. The method applicability was studied by analyzing samples of water, seawater, tap water and well water. The samples were collected in polypropylene bottles treated as described in section 2.2. These waters were immediately filtered employing a cellulose nitrate filters membrane with a pore size of $0.45 \mu\text{m}$ from Millipore (Bedford, MA, USA) and acidified to 0.1% (wt/wt) by adding of concentrated HNO_3 and were stored at 4°C for less than 3 days, as commended by Method 3010 B from the Environmental Protection Agency (USA). For sample preparation, aliquots of samples were placed in volumetric flasks, then the pH was set at 3 with glycine/HCl buffer (adding 10% of the total volume), and ultimately, DDW was added up to the mark. For the seawater samples, the conductivity was adjusted with NaCl so that standards and samples showed the same salinity.

2.4. Preconcentration and elution procedure

Fig. 1 shows a description of the MSPE-ICP-OES system. Table 1 shows the optimal experimental conditions. The system works as follows: Initially, the valve is in position A, sample loading period, the samples at pH 3.0 (std or blank) are pumped (via pump P1) through the

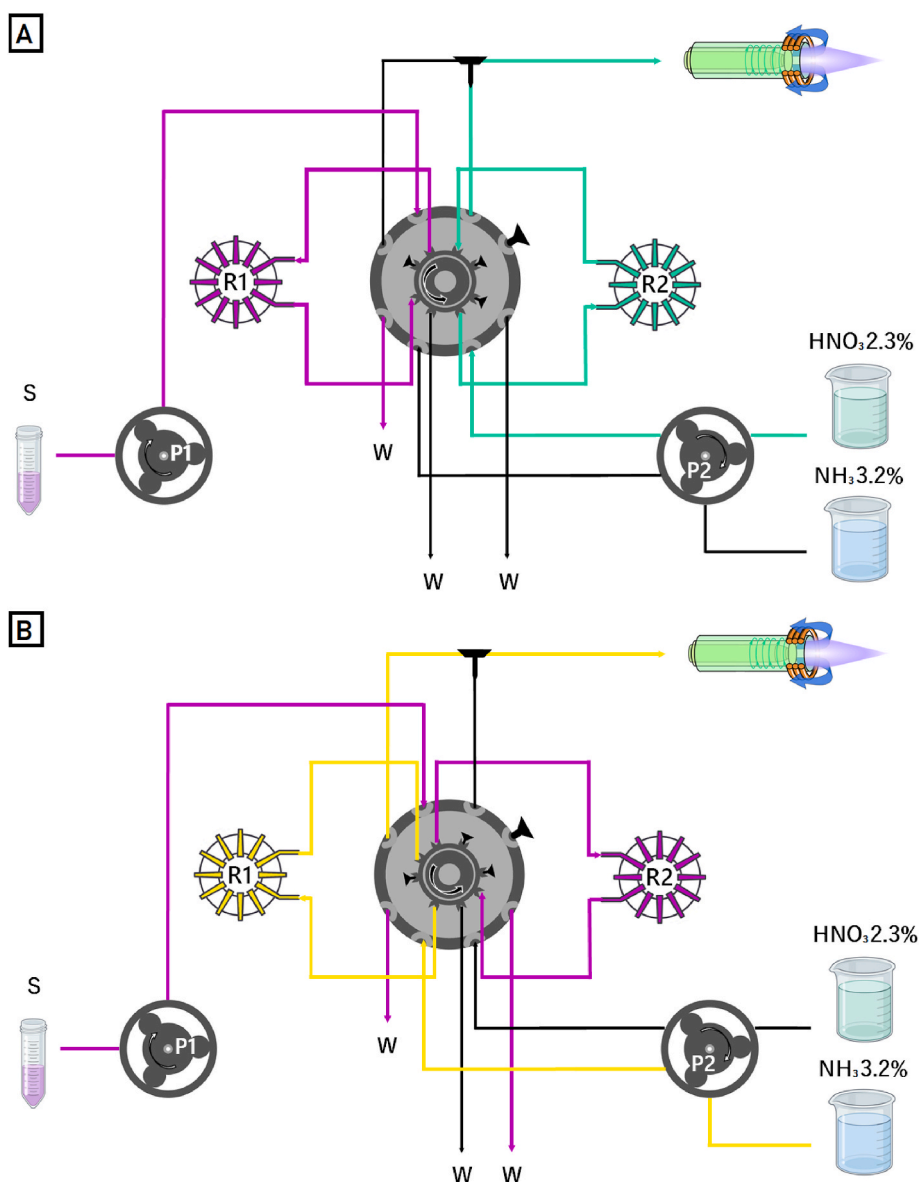


Fig. 1. Graph of the MSPE-ICP-OES system for the preconcentration and separation of chromium; P1 and P2, peristaltic pumps; S Sample, W Waste, R1 and R2 knotted reactors at both available positions A and B.

reactor R1 at 1.3 mL min^{-1} for 180 s. The Cr(III) and Cr(VI) analyte species are retained on the M@GO-ABS, while the sample matrix components are wasted. After that (second step), to clean matrix components, DDW was pumped through R1 for 30 s (via pump P1) at a flow rate of 1.5 mL min^{-1} .

At the third step, the valve is changed to the position B. Then, a 3.2% NH_4OH solution at 3 mL min^{-1} is passed through the R1 in reverse flow relative to the preconcentration step (preventing the compactness of the reactor). Thus, Cr(VI) was eluted from R1 and pumped to the ICP-OES. At the same time, during other 180 s sample (std or blank) at pH 3.0 and a flow rate of 1.3 mL min^{-1} was pumped (via pump P1) through the R2 (located in the second loop of the valve). After that (fourth step), to clean the matrix components, DDW was pumped through the R2 during 30 s (via pump P1) and at a 1.5 mL min^{-1} flow rate. At the fifth step, total Cr accumulated in R2 was eluted at a flow rate of 4.2 mL min^{-1} with 2.3% HNO_3 and pumped to the ICP-OES while R1 was also cleaned with HNO_3 (2.5 mL min^{-1}), leaving the knotted reactors ready for a new sample loading period.

Both eluting solutions were swept into the plasma by a stream of argon (0.7 L min^{-1}). The waste was drained through the peristaltic pump of the ICP-OES at a flow rate of 4 mL min^{-1} . This procedure is performed in triplicate.

The instrument software provides information of the measured transient signals, such as peak height and peak area. Peak height showed higher sensitivity and precision. Therefore, peak height was selected and used for quantification.

2.5. Optimization plan

To reach the best results, both the MSPE-ICP-OES system configuration and the effects of the different parameters involved in the accumulation and recovery of both Cr species were optimized. For that, a standard solution with a concentration of $300 \mu\text{g L}^{-1}$ of Cr(VI) and $300 \mu\text{g L}^{-1}$ of Cr(III) and a blank were prepared. Optimization was carried out using: a one-at-a-time method (changing one parameter at a time and keeping the others constant); and surface designs with multiple responses. The response functions were the signal-to noise ratio for Cr (VI) and total Cr.

Many parameters are important for the optimization and are classified as chemical and instrumental parameters: *chemical*, (1) pH, (2) eluents concentration; and *instrumental*, (3) FI parameters and (4) ICP-OES conditions. For (1) and (4) a one-at-a-time strategy was used; for (2) and (3) two surface designs were performed.

In design (2), eluent solutions, the concentrations of HNO_3 and NH_4OH , were optimized. The lower and upper values given to each factor were 0.0% and 5.0% concentration. In design (3), all the previously optimized variables were kept constant (pH 3, 3.2% NH_4OH and 2.3% HNO_3), and the sample and elution flow rates were varied by changing the speed of the peristaltic pumps (P1 and P2) and the inner diameter of the pump tubes. The lower and upper values given to each factor were $0.6\text{--}4.2 \text{ mL min}^{-1}$ for the elution flow rates of HNO_3 and NH_4OH , and $0.6\text{--}5 \text{ mL min}^{-1}$ for sample flow rate. The used response surface designs were two central composite designs (CCD) for (2) and (3). The 10 and 16 required experiments, respectively, for these designs were accomplished arbitrarily. The response functions to be maximized were both the signal-to-noise ratio for the Cr(VI) and the signal-to-noise ratio for the total Cr.

Statgraphics Centurion program (version 16.1.11 for Windows) was used to process the experimental data. The significance of the effects was tested by analysis of variance (ANOVA) and utilizing *p-value* significance levels in both cases. This value signifies the probability of the effect of a factor being due exclusively to arbitrary error. Thus, if the *p-value* is less than 5%, the effect is significant.

2.6. Synthesis of the functionalized M@GO

The synthesis of M@GO was reported in the patent [18,20].

The obtained M@GO was functionalized in several steps. The M@GO was first suspended in 50 mL of ethanol with 8 mL of EDA and 250 mg of DCC in a round bottom flask, heated at $50 \text{ }^\circ\text{C}$ for 48 h. The suspension was naturally cooled down to room temperature and magnetically decanted, and then washed with doubly de-ionized water and ethanol. Subsequently, it was left to dry for 72 h in a desiccator. Afterwards, 500 mg of this dry solid were introduced into a round bottom flask where 50 mL of a 1% glutaraldehyde solution in ethanol and 10 drops of glacial acetic acid were added, the mixture was heated under reflux for 4 h, then the solid was magnetically separated from the matrix and washed with deionized water. Finally, 50 mL of a 2% sulfanilic acid solution in ethanol was added to the flask and the mixture was heated under reflux for 24 h. Then, the solid was separated and washed with DDW and left to dry for 72 h.

As shown in Fig. 2, this functionalization introduces N and S into the sorbent, presenting pairs of free electrons which can interact with metals, giving place to coordination complexes, in addition to a sulfonic group that can interact with cations. Furthermore, the metal chelation in these complexes is influenced by pH, since all the complexes have an optimum pH for formation. Thus, by varying the pH of the solution, it is possible to separate the metal from the sorbent.

2.7. Analysis of the adsorption capacity

The adsorption capacity of the novel magnetic nanosorbent by Cr(III) and Cr(VI) was studied. To evaluate the M@GO-ABS adsorption capacity, an in batch MSPE procedure was carried out, determining Cr(III) and Cr(VI) in the supernatant by ICP-Mass Spectrometry (ICP-MS). The adsorption capacity depends on the pH, so pH 5 and 8 were checked. Standard solutions of $50 \mu\text{g L}^{-1}$ of Cr(III) and Cr(VI) were prepared in four 50 mL volumetric flasks at the two pHs by adding 10% of the total volume (5 mL) of buffers $\text{CH}_3\text{COOH}/\text{CH}_3\text{COONa}$ for pH 5 and $\text{H}_3\text{BO}_3/\text{Na}_2\text{B}_4\text{O}_7 \cdot 10\text{H}_2\text{O}$ for pH 8. Next, 5 mg of M@GO-ABS were weighed in four 100 mL beakers. The M@GO-ABS was scattered by ultrasonication for 10 min at room temperature and afterwards magnetically separated. The Cr(III) and Cr(VI) were measured in the supernatants meaning no extracted metal ions. The adsorption capacity for each species was estimated by the difference between the initial and final concentration in the supernatants.

3. Results and discussion

3.1. Characterization of M@GO-ABS

For the characterization of M@GO-ABS measurements of XPS, FTIR and TEM were performed. The supplementary material (SM) shows the tables and figures obtained in the material characterization.

TEM. The structure and surface morphology of the synthesized M@GO-ABS were studied by TEM (Fig. SM1). Nanosheets of GO can be observed. The MNPs have been correctly dispersed on the GO sheets. This dispersion is random, presenting areas with greater aggregation of nanoparticles and areas in which no coupling has occurred.

Elemental Analysis. TEM images show the presence of carbon and oxygen indicating the existence of graphene oxide in the synthesized material. And the presence of S indicates that the functionalization of GO has been carried out correctly, since S comes from the functionalization with the sulfanilic group, Table 2.

XPS analysis. The XPS spectra of M@GO-ABS in the region of N and S, respectively, are shown in SM2 and SM3. In SM2 a peak appears for S (2p) at 168 eV, corresponding to the sulfonic group. In SM3, a double peak appears for N(1s). The peak at 399 eV corresponds to the aromatic nitrogen [18] while the peak at 402 eV is due to ammonium salts [18] $\text{NH}_4^+\text{SO}_3^-$.

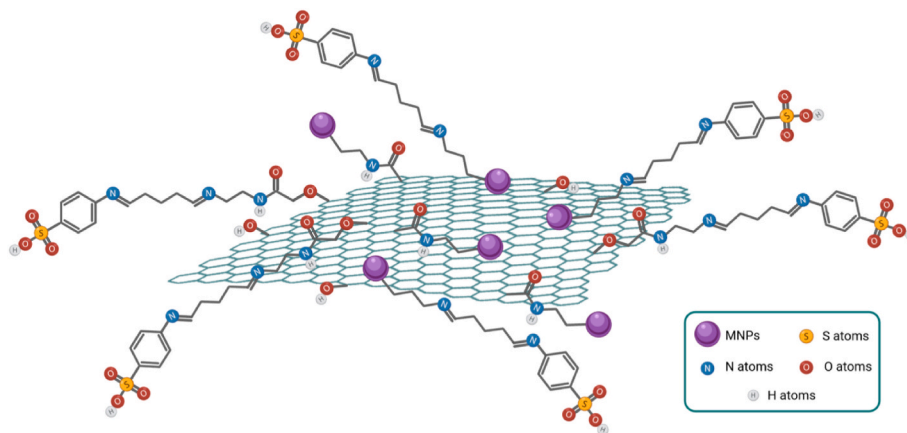


Fig. 2. Functionalized MGO, M@GO-ABS.

Table 2
Elemental analysis.

Sample	%C	%O	%H	%N	%S
M@GO-ABS	53.82	25.24	3.63	4.51	1.18

From XPS analysis, the atomic percentage for M@GO-ABS is reported in Table 3.

The high percentage of C and O stands out, confirming the existence of GO in the material, Fe confirms the presence of MNPs, and the presence of N and S confirms the correct functionalization.

FT-IR. The FT-IR spectrum (KBr pellets) shows numerous bands due to the aromatic portion of the molecules that overlap making it difficult to assign. Nevertheless, several assignments were done in the mid-infrared region (Fig. SM4). In the 1450–1600 cm^{-1} area an overlap was observed between the amide II bands and the aromatic skeletal bands, the latter together with those of $\nu_{(\text{SO})}$, $\nu_{(\text{SO}_2 \text{ s})}$ and $\nu_{(\text{SO}_2 \text{ as})}$ suggested that the material has been correctly functionalized with sulfonic acid. In M@GO-ABS was shown a band at 1350 cm^{-1} due to $\nu_{(\text{S}=\text{O})}$. The $\nu_{(\text{SO}_2 \text{ s})}$ and $\nu_{(\text{SO}_2 \text{ as})}$ bands appeared about 1000 cm^{-1} , and $\nu_{(\text{SO})}$ appeared in the 500–600 cm^{-1} .

In the 1110–1200 cm^{-1} band, two peaks can be distinguished, $\nu_{(\text{COC s})}$ and $\nu_{(\text{COC as})}$ which are overlapping and cannot be distinguished separately. The existence of the $\nu_{(\text{C}=\text{O})}$ at 1701 cm^{-1} bands indicate that the modification made on the GO has been carried out correctly. The band $\nu_{(\text{C}=\text{N})}$ at 1701 cm^{-1} indicates the existence of imino groups corresponding to the last stage of the functionalization process and to the reaction of EDA and glutaraldehyde.

The $\nu_{(\text{Fe}-\text{O})}$ band at 600 cm^{-1} suggests that the dispersion of iron nanoparticles in GO has occurred correctly, although that band is not as intense as expected due to the chosen M@GO synthesis methodology. The low level of iron can be explained by considering the possible oxidation of iron species in the synthesis of M@GO. This could be due to the interaction with the oxygenated surface of GO. The success of the synthesis and functionalization is corroborated with all these studies.

Nitrogen Adsorption/Desorption Isotherms. The nitrogen adsorption-desorption experiment presented isotherm like those type IV, typical of mesoporous materials (pore size between 20 and 500 Å) [21–23,].

The isotherm of M@GO-ABS material is in Fig. SM5. Some physics

Table 3
Analysis of C, N, O, S and Fe obtained from XPS.

%C	%N	%O	%S	%Fe
64.52	4.05	23.41	2.53	4.06

characteristics of the materials are a pore size of 103 Å and a surface area of 16.3 $\text{m}^2 \text{g}^{-1}$. As can be seen, the materials are mesoporous and present a surface area higher than uncoupled GO (2.63 $\text{m}^2 \text{g}^{-1}$).

Mass Spectrometry. The characteristic peaks observed in the MS spectra, were assigned to different fragments. The most relevant peaks are indicated in Table 4.

3.1.1. Adsorption capacity of the M@GO-ABS material

The adsorption capacity of the nanosorbent was studied in batch process as described in 2.7. section. The adsorption capacity of the material for each species was estimated from the difference between the metal ion concentrations in the solution before and after sorption. The estimated adsorption capacity for each species at pH 3, 5 and 8 is shown in Table 5.

3.2. Optimization plan

To achieve compromise conditions for simultaneous determination of both species, some of the parameters were optimized in a univariate way, e.g. pH and others using some multiple response central composite designs.

3.2.1. Influence of pH

The influence of pH on the adsorption of the species in the M@GO-ABS was first studied, since the pH affects the complexation of the ions with the material, to locate a pH that would allow the two species to be discriminated. For the optimization, standard solutions of 300 $\mu\text{g L}^{-1}$ of Cr(III) and Cr(VI) were prepared at different pHs in the range between 1.0 and 11.0, Fig. 3. The $\text{pH} \leq 2$ was adjusted with diluted hydrochloric acid; from 2.0 to 6.0 were adjusted using glycine–hydrochloric acid and

Table 4
MS-Identification of some peaks of M@GO-ABS.

Peak (m/z)	Fragment
39	
44	$\text{O}=\text{C}-\text{NH}_2^+$
64	SO_2^+
93	
281	

Table 5
Adsorption capacity.

Element	Adsorption capacity (mg g ⁻¹)
Cr(III) pH 3	0.36
Cr(III) pH 5	0.27
Cr(III) pH 8	0.21
Cr(VI) pH 3	0.35
Cr(VI) pH 5	0.27
Cr(VI) pH 8	0.30

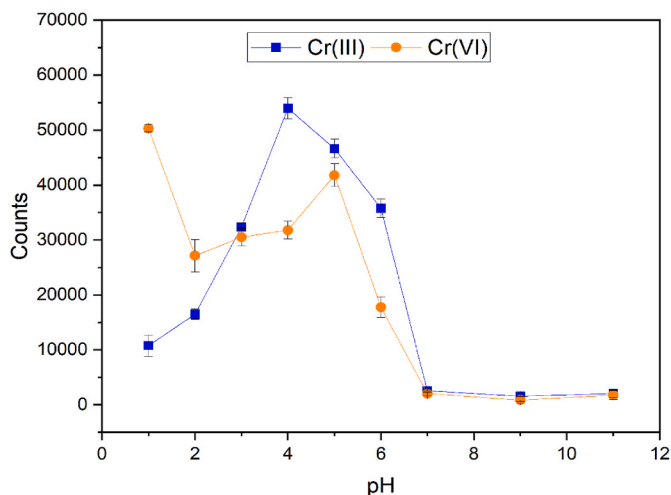


Fig. 3. Study of pH on the speciation of chromium.

CH₃COOH/CH₃COONa buffers; from 7.0 to 11.0 employing H₂PO₄⁻-HPO₄²⁻ and NaOH-HPO₄²⁻ buffers.

As it can be observed in Fig. 3, only at pH 1 the behaviour of both species is different. Although, the Cr(III) signal is small compared to Cr(VI) signal, the selectivity towards Cr(VI) is compromised, so it cannot be used for the selective determination of only a chromium species. On the other hand, both chromium species are better adsorbed at pH between 3 and 5. Finally, pH 3 was selected as optimum because both signals are similar.

3.2.2. Effect of eluent

The speciation cannot be achieved at any pH according to the pH curves. Thus, three different possibilities were considered; the use of selective eluents for Cr(III) such as potassium phthalate [24] or 1,1,1-trifluoroacetone [25], the use of selective eluents for Cr(VI) such as 1,5-diphenylcarbazide (DPC) [26] or ammonia, and the transformation of one species into another by chemical reaction. In this case, the concentration of both species could be obtained by the difference between total chromium and the eluted species [27]. Due to the toxic nature of Cr(VI), eluents that were selective for that species were considered. As it is known, ICP-OES is little tolerant to organic eluents, so ammonia was tested as eluent for Cr(VI). Moreover, the decision was reinforced by the composition of sorbent materials for Cr(VI) described in bibliography [28].

The obtained results for ammonia were positive, Cr(VI) was selectively eluted when the eluent was NH₄OH. This effect may be explained because at high pHs Cr(III) forms its hydroxide Cr(OH)₃ which precipitates and is not eluted [23].

HNO₃ was observed to elute both chromium species, while using NH₄OH as eluent, only Cr(VI) was eluted. Thus, the speciation was possible at pH 3 using both eluents, and a two reactors system, Fig. 1. Both reactors are loaded at the same time, while for the elution step, one reactor was eluted with NH₄OH and the other one with HNO₃.

A CCD involving 10 runs was performed to study the concentrations

of HNO₃ and NH₄OH, dependent variables and therefore their effects have to be studied in order to obtain the optimal conditions for the speciation based on maximizing both, the signals for the Cr(VI)/noise and the signals for total Cr/noise, meaning the best signal-to-noise (S/N) ratios were chosen as the optimization criterion (Desirability). The three-dimensional response surface shows the desirability versus HNO₃ and NH₄OH concentrations, Fig. 4.

The best S/N signals were achieved with 3.2% NH₄OH and 2.3% HNO₃, being the optimal eluent conditions.

3.2.3. Effect of sample and eluents flow rate

The preconcentration factor is strongly influenced by the eluent volume, therefore the eluent flow rates must be as low as possible to obtain the maximum enrichment factor values. On the other hand, the sample flow rate should be optimized to ensure quantitative retention along with minimization of the required time for sample processing.

The sample and eluent flow rates are two important factors for the quantitative recoveries and desorption of species at SPE. To investigate the effects a multiple response CCD involving 16 runs was designed. Based on the results provided by the Statgraphics software, the optimal conditions were sample flow rate of 0.6 mL min⁻¹, NH₄OH eluent flow rate of 3.2 mL min⁻¹, and HNO₃ eluent flow rate of 2.3 mL min⁻¹, Fig. 5.

The optimized sample flow rate was low, this is logical because the sorbent has a greater facility to retain the analytes with longer contact time. However, a higher sample flow leads to higher signals. Therefore, an additional series of experiments were developed to study the influence of the flow rate on the signal, using a constant sample volume as a condition. Different flow rates were studied (0.60, 1.30, 2.40, 3.15 and 5 mL min⁻¹), and an increase in the signal was observed up to 1.3 mL min⁻¹. Furthermore, very high flow rates represent a potential risk in the FI system, since the connections can be overpressured. Thus, the chosen sample flow rate was 1.3 mL min⁻¹.

The reactors must be washed after the sample loading to remove sample matrix residues that could be present in the dead volume of the reactor and could represent a potential source of error. For removing the matrix elements, the reactors were washed with DDW, at a flow rate between 0.8 and 1.8 mL min⁻¹ and washing time between 30 s and 60 s. In general, the results were similar and a washing time of 30 s with DDW using a flow rate of 1.8 mL min⁻¹ was selected, since that was the minimum time that allowed the volume of the knotted reactor to be complete.

3.2.4. Preconcentration time

The loading or preconcentration time directly affects the enrichment factor and the sensitivity. The sensitivity increased on increasing the preconcentration time, nevertheless the sampling frequency decreased. That time was researched between 60 s and 300 s for each Cr(VI) and total Cr, maintaining the optimal conditions described above. The signals intensities increased almost linear up to 5 min for both analytes. To achieve a compromise situation, the preconcentration time was set to 180 s, which allowed a high sampling frequency with satisfactory sensitivity (if higher sensitivity was required due to low analyte concentrations, the preconcentration time could be increased). In Fig. 6 the FI-graph with the optimal conditions for the analysis of a standard containing 300 µg L⁻¹ of Cr(VI) and 300 µg L⁻¹ of Cr(III), and 180 s preconcentration time is shown.

3.2.5. Study of the ICP operating parameters

The influence of the nebulizer gas flow rate and radiofrequency were investigated. The nebulizer gas affects transport. Taking into account the optimal conditions described above, the Ar flow rate was examined. A standard solution and a blank were measured. The Ar flow rate was investigated between 0.2 and 1.0 L min⁻¹, and a maximum signal to noise ratio was found at a flow rate of 0.6 L min⁻¹.

For the optimization of the radiofrequency, trials were carried out at 1300, 1400 and 1500 MHz, a standard solution and a blank were

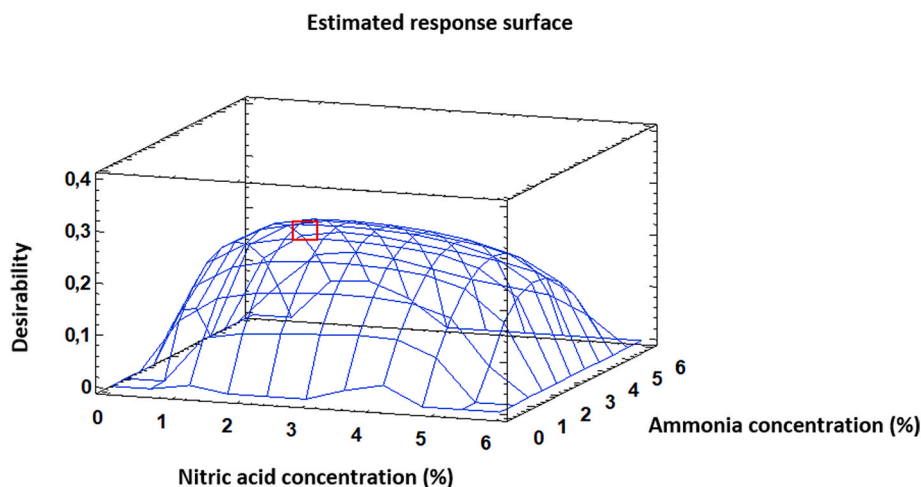


Fig. 4. Response surface obtained for Cr(III) and Cr(VI) analytes.

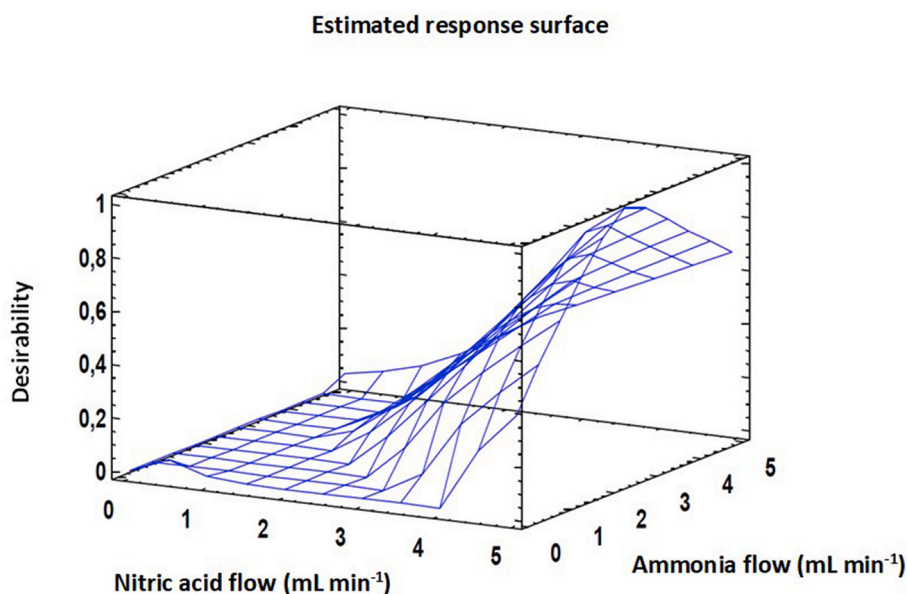


Fig. 5. Response surface obtained for Cr(III) and Cr(VI) analytes.

measured. At 1400 MHz, the signals, especially Cr(VI) were enhanced. Thus, the 1400 MHz was selected as optimum.

3.3. Performance of the method

Establishing the optimal conditions described previously, the performance data of the on-line MSPE-ICP-OES system for determination of Cr(VI) and total Cr were obtained. For 3 min preconcentration time and a sample flow rate of 1.3 mL min^{-1} , a linear calibration graph for Cr(VI) and total Cr was obtained. The equations for calibration curves, blank signals, limits of detection and quantification (LODs and LOQs) and other analytical characteristics are presented in Table 6.

A complete cycle of the FI-operation was ca. 480 s per sample, the speciation of Cr in a sample can be established with a throughput of $7,5 \text{ h}^{-1}$.

The limits of detection (LOD) and quantification (LOQ) were calculated as the concentration of Cr(III) and Cr(VI) giving signals equivalent to three and ten times ($n = 11$), respectively, the standard deviation of the blank plus the net blank intensity; the precision for aqueous standards was estimated as the relative standard deviation calculated after

analyzing a standard of $5 \mu\text{g L}^{-1}$ of Cr(VI) and $10 \mu\text{g L}^{-1}$ total Cr (7 replicates), $50 \mu\text{g L}^{-1}$ of Cr(VI) and $100 \mu\text{g L}^{-1}$ total Cr (11 replicates), $300 \mu\text{g L}^{-1}$ of Cr(VI) and $600 \mu\text{g L}^{-1}$ total Cr (8 replicates) and the enrichment factor EF, defined as the ratio of the slopes of the linear section of the calibration graphs with and without preconcentration (changing the R by another empty). The EFs and determination limits can be improved by increasing the preconcentration time which can be increased at least up to 5 min.

The lifetime of a R filled with 50 mg of M@GO-Abs was studied and was concluded that was useful for 200 measurements without refilled. The performance data for the most toxic species, Cr(VI), of comparable methods described in the bibliography are shown in Table 7. The comparison between the other works and proposed the method is difficult due to different experimental conditions such as type of packing, quantity of sorbent, sample flow rate, etc. Nevertheless, the detection limits and the precision of the proposed method were better than or similar to those described in the bibliography. The proposed method allows the analysis of both chromium species in an easy, fast and totally automatic way. Comparing our method with the last one which is a very recent publication, the detection limits and precisions are similar, being

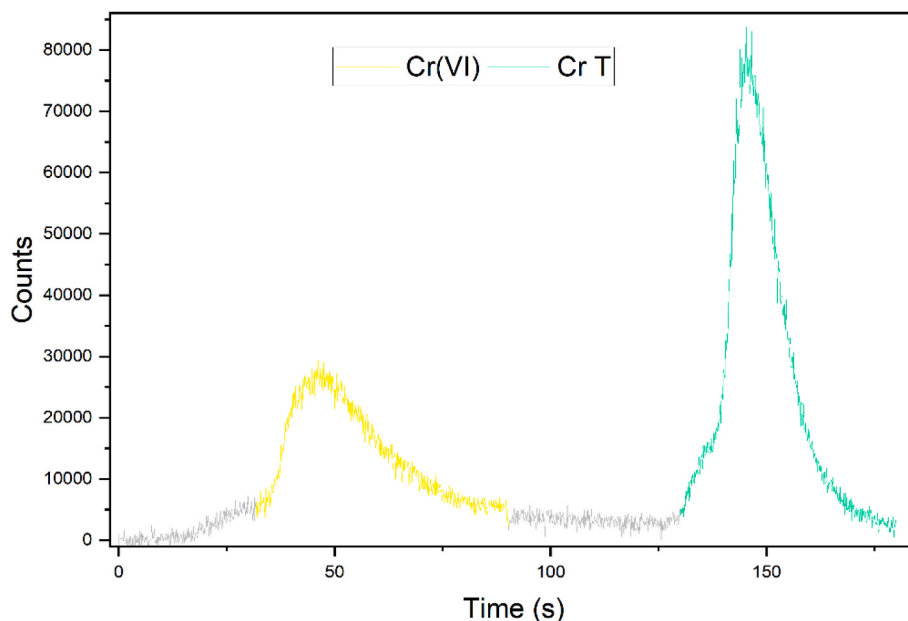


Fig. 6. ICP-OES signals for 300 $\mu\text{g L}^{-1}$ of Cr(III) and 300 $\mu\text{g L}^{-1}$ Cr(VI).

Table 6
Analytical performance.

Species	Calibration graph	Blank \pm S_b N = 11	LOD ($\mu\text{g L}^{-1}$)	LOQ ($\mu\text{g L}^{-1}$)	RSD (%) 5 $\mu\text{g L}^{-1}$ N = 7	RSD (%) 50 $\mu\text{g L}^{-1}$ N = 11	RSD (%) 300 $\mu\text{g L}^{-1}$ N = 8	Enrichment Factor
Cr(VI)	$y = 1141.6x + 949.2$	472 ± 198	0.1	1.31	4.7	6.7	3.9	15
Cr T	$y = 2220.3x + 435.3$	12 ± 205	0.08	0.73	4.2	8.4	3.3	23

Table 7
Comparison of analytical performance data with other data reported in the literature.

Sample	Technique	Sorbent	LOD ($\mu\text{g L}^{-1}$)	EF	RSD	Ref.
Eyes shadow	ICP-OES	Na_3PO_4	0.15	–	10.1	[22]
Sea water	FAAS	Potassium phthalate	75	0.94	3.4	[23]
Sea water	FAAS	DOWEX-1	0.037	10	–	[28]
Aq. standards	CPE-HPLC	Triton X-114	5.2	19	4.2	[15]
River water	ICP-OES	Iminodiacetate	0.15	5.1	5.5	[29]
Physiological serum	FAAS	SiO_2 -AAPTMS	0.66	17.6	2.4	[30]
Aq. standards	ICP-OES	TiO_2	1.52	26	2.4	[31]
Water	FAAS	PS-NAPdien	2.5	30	0.8	[32]
Tap and river water	AAS	Dowex M4195	1.94	31	10	[33]
Water	FAAS	Amberlite XAD-16	45	25	3	[34]
Water	FAAS	PMA and PVI	1.58	8.6	–	[35]
Water	FAAS	<i>Moringa oleifera</i> husks	2.45	–	1.63	[36]
Water	FAAS	$\text{Fe}_3\text{O}_4/\text{SiO}_2$	1.1	16	5.5	[37]
Environmental water	FAAS	mf-GO	1.4	10	5	[38]
Environmental samples	ICP-OES	Fe_3O_4 SiO_2 GO AIL	0.19	2.6	4.9	[39]
Tannery wastewater	FAAS	Amborsorb 563	2.70	–	<10	[40]
Environmental samples	FAAS	CFMEPI	0.7	40	<7	[41]
Tap, well and sea water	ICP-OES	M@GO-ABS	0.1	14	6.7	This work

the main difference that the proposed method is totally automatic, the fastest one, the sequential determination of both species needs only 8 min, and the consumption of sample and reagents are much less. In addition, it is the only one that has been applied to the speciation in seawater (one of the most complex matrices that exists).

Using 180 s as loading time, the sample consumption for each knotted reactor is 3.9 mL ($1.3 \text{ mL min}^{-1} \times 3 \text{ min}$) and only 50 mg of M@GO-ABS were needed for 200 measurements. The low consumption of sample and reagent fits the proposed method within the Green Analytical Chemistry.

3.4. Analytical application

The developed method was validated by determining two certified reference materials, TMDA 54.5 Fortified Lake Water and SPS-SW2 surface waters, and real samples as: tap water, well water, sea water. The analyses of all samples ($n=3$) were performed by an external standard calibration. The results as the average of four separate determinations are shown in Table 8, no significant differences were detected, for $p=0.05$ when comparing the values obtained by the developed method and certified values (t -test for a 95% confidence level

Table 8
Analytical applications.

Sample	Cr total certificate ($\mu\text{g L}^{-1}$)	Added ($\mu\text{g L}^{-1}$)		Found ($\mu\text{g L}^{-1}$)			Recovery (%)		
		Cr(III)	Cr(VI)	Total Cr	Cr(VI)	Cr(III)	Cr(III)	Cr(VI)	Total Cr
SPS-SW2	10 \pm 0.05	–	–	9.6 \pm 0.2	7.1 \pm 0.3	2.55 \pm 0.05	–	–	–
		50	50	116 \pm 2	60 \pm 3	56.0 \pm 0.9	107	106	109
		100	100	197 \pm 3	99 \pm 4	98 \pm 2	95	92	95
TMDA	282 \pm 18	–	–	290 \pm 3	<LOD	290 \pm 3	–	–	–
		50	50	400 \pm 9	54 \pm 2	346 \pm 7	112	108	110
		100	100	500 \pm 10	99 \pm 5	401 \pm 9	111	99	105
Tap water	–	–	–	5.1 \pm 0.1	3.4 \pm 0.2	1.70 \pm 0.05	–	–	–
		50	50	103 \pm 3	54 \pm 6	49 \pm 1	95	101	98
		200	200	410 \pm 25	210 \pm 6	200 \pm 10	99	103	101
Water well	–	–	–	54 \pm 3	17 \pm 1	37 \pm 2	–	–	–
		200	200	420 \pm 20	199 \pm 4	221 \pm 1	92	91	92
		300	300	640 \pm 40	300 \pm 8	340 \pm 20	101	94	98
Sea water GM	–	–	–	37.8 \pm 0.9	19.5 \pm 0.3	18.3 \pm 0.5	–	–	–
		100	100	243 \pm 2	117 \pm 9	126 \pm 1	108	98	103
		200	200	427 \pm 5	215 \pm 9	212 \pm 3	97	98	97
Sea water TX	–	–	–	25 \pm 1	17.7 \pm 0.7	7.3 \pm 0.3	–	–	–
		200	200	390 \pm 20	200 \pm 10	190 \pm 10	91	91	91
		300	300	600 \pm 30	300 \pm 10	300 \pm 20	98	94	96

($t_{\text{calculated}} = -0.90$ and $t_{\text{tabulated}} = 12.70$)).

Since the certified reference materials have included trace elements, it can be assumed that the method does not present any metal interferences at $\mu\text{g L}^{-1}$ concentrations. Furthermore, an alternative validation process was performed as recovery tests, Table 8. The recoveries for the spiked samples were close to 100%. These outcomes reveal that the proposed method is useful to apply to the speciation of Cr in samples with very complex matrix such as sea water (high salinity about 35.5 g L^{-1}).

4. Conclusion

An on-line preconcentration and separation method utilizing a novel functionalized magnetic nanomaterial, M@GO-ABS, as a sorbent material has been assessed and proved to be promising for the speciation of Cr in environmental waters by ICP-OES. The proposed method has proven to be automatic, high-speed, selective, unexpensive and uncomplicated, also showing very good analytical characteristics. The good analytical characteristics of the proposed method make it suitable for the determination of trace amounts of Cr(III) and Cr(VI) in environmental samples. The comparison, Table 7, has demonstrated that the proposed method has a good sensitivity and precision, with LOD and LOQ of 0.1 $\mu\text{g L}^{-1}$ for Cr(VI) and 0.088 $\mu\text{g L}^{-1}$ for total Cr, and 1.31 $\mu\text{g L}^{-1}$ for Cr(VI) and 0.73 $\mu\text{g L}^{-1}$ for total Cr, respectively, being one of the best methods for the speciation of Cr. The method was validated by the analysis of Certified reference materials (TMDA 54.5 fortified lake water and SPS-SW2 surface water) and spiked aqueous, and the analysis was performed with external calibration of Cr(III) and Cr(VI) spiked environmental water samples including seawater. The relative recoveries were between 91 and 112%, showing the selectivity of the method because these samples have complex and highly saline matrices including trace elements such as transition metals.

The MSPE system offers a few advantages such as simplicity of operation, high sample throughput, and reduced sample and reagent consumption (in this case, 7.8 mL, 5.5 mL (NH_4OH) 6.7 mL (HNO_3) of eluent, per replicate).

Author contributions

E. I. Vereda Alonso: conceptualization, methodology, formal analysis, writing – original draft, writing – review & editing, software, data curation, supervision, resources, funding acquisition. **M. M. Lopez Guerrero:** conceptualization, methodology, formal analysis, writing – original draft, writing – review & editing, data curation, supervision,

resources. **I. Morales Benítez:** investigation, methodology, writing – review & editing, software, formal analysis, data curation. **P. Montoro Leal:** investigation, methodology, writing – review & editing, software, formal analysis, data curation. **J. C. Garcia-Mesa:** investigation, methodology, validation, software, formal analysis, writing – review & editing, data curation. All authors have read and agreed to the published version of the manuscript.

Declaration of competing interest

The authors declare that they have no known competing financial interests or personal relationships that could have appeared to influence the work reported in this paper.

Data availability

Data will be made available on request.

Acknowledgements

The authors thank the University of Malaga (Proyecto Puente B4-2021-10 and predoctoral grant A.2.2021) and Spanish Ministerio de Ciencia e Innovación, Project PID2021–126794OB-100 for supporting this study and the Spanish Ministerio de Ciencia y Tecnología for the fellowship FPU18/05371. The authors would like to thank Dra. Mónica Giménez Lazarraga for the English revision. Funding for open access charge: Universidad de Málaga/CBUA.

Appendix A. Supplementary data

Supplementary data to this article can be found online at <https://doi.org/10.1016/j.talanta.2023.124262>.

References

- [1] A. Gonzalez, M.L. Cervera, S. Armenta, M. de la Guardia, A review of non-chromatographic methods for speciation analysis, *Anal. Chim. Acta* 636 (2009) 129–157, <https://doi.org/10.1016/j.aca.2009.01.065>.
- [2] J.M. Lavelle, Mechanisms of toxicity/carcinogenicity and superfund decisions, *Environ. Health Perspect.* 92 (1991) 127–130, <https://doi.org/10.1289/ehp.9192127>.
- [3] M.F. Bergamini, D.P. dos Santos, M.V.B. Zanoni, Development of a voltammetric sensor for chromium(VI) determination in wastewater sample, *Sensor. Actuator. B Chem.* 123 (2007) 902–908, <https://doi.org/10.1016/j.snb.2006.10.062>.
- [4] A. Kot, J. Namiesnik, The role of speciation in analytical chemistry, *TrAC, Trends Anal. Chem.* 19 (2000) 69–79, [https://doi.org/10.1016/S0165-9936\(99\)00195-8](https://doi.org/10.1016/S0165-9936(99)00195-8).

- [5] S. Kalidhasan, A. Santhana Krishna Kumar, V. Rajesh, N. Rajesh, The journey traversed in the remediation of hexavalent chromium and the road ahead toward greener alternatives-A perspective, *Coord. Chem. Rev.* 317 (2016) 157–166, <https://doi.org/10.1016/j.ccr.2016.03.004>.
- [6] J. Guertin, J.A. Jacobs, C.P. Avakian, *Chromium (VI) Handbook*, first ed., CRC Press, Florida, 2005 <https://doi.org/10.1201/9780203487969>.
- [7] World Health Organization, *Chromium in Drinking-Water*, World Health Organization, 2020. No. WHO/HEP/ECH/WSH/2020.3.
- [8] G. Howells, *Chemical speciation in the environment*, *Chem. Ecol.* 11 (1995) 135–136, <https://doi.org/10.1080/02757549508037695>.
- [9] R. Cornelis, *Handbook of Elemental Speciation: Techniques and Methodology*, John Wiley & Sons, Ltd, Great Britain, 2003, <https://doi.org/10.1002/0470868384>.
- [10] G. Howells, 11:2, in: A.M. Ure, C.M. Davidson (Eds.), *Chemical Speciation in the Environment*, Hardback, Chemistry and Ecology, Blackie Academic and Professional, Chapman and Hall, London, 1995, ISBN 0 7514 0021 1, pp. 135–136, <https://doi.org/10.1080/02757549508037695>. Library of Congress Cat. No.: 94 71807, 408 1995.
- [11] W. Alahmad, N. Tungkiyanansin, T. Kaneta, P. Varanusupakul, A colorimetric paper-based analytical device coupled with hollow fiber membrane liquid phase microextraction (HF-LPME) for highly sensitive detection of hexavalent chromium in water samples, *Talanta* 190 (2018) 78–84, <https://doi.org/10.1016/j.talanta.2018.07.056>.
- [12] A. Shishov, P. Terno, L. Moskvina, A. Bulatov, In-syringe dispersive liquid-liquid microextraction using deep eutectic solvent as disperser: determination of chromium (VI) in beverages, *Talanta* 206 (2020) 1–7, <https://doi.org/10.1016/j.talanta.2019.120209>.
- [13] A. Ghiasi, A. Malekpour, Octyl coated cobalt-ferrite/silica core-shell nanoparticles for ultrasonic assisted-magnetic solid-phase extraction and speciation of trace amount of chromium in water samples, *Microchem. J.* 154 (2020) 1–9, <https://doi.org/10.1016/j.microc.2019.104530>.
- [14] M. Shirani, F. Salari, S. Habibollahi, A. Akbari, Needle hub in-syringe solid phase extraction based a novel functionalized biopolyamide for simultaneous green separation/preconcentration and determination of cobalt, nickel, and chromium (III) in food and environmental samples with micro sampling flame atomic absorption spectrometry, *Microchem. J.* 152 (2020), 104340, <https://doi.org/10.1016/j.microc.2019.104340>.
- [15] A.N. Tang, D.Q. Jiang, Y. Jiang, S.W. Wang, X.P. Yan, Cloud point extraction for high-performance liquid chromatographic speciation of Cr(III) and Cr(VI) in aqueous solutions, *J. Chromatogr. A* 1036 (2004) 183–188, <https://doi.org/10.1016/j.chroma.2004.02.065>.
- [16] M. Hemmati, M. Rajabi, A. Asghari, Magnetic nanoparticle based solid-phase extraction of heavy metal ions: a review on recent advances, *Microchim. Acta* 185 (2018) 160–192, <https://doi.org/10.1007/s00604-018-2670-4>.
- [17] A.E. Karatapanis, Y. Fiamegos, C.D. Stalikas, Silica-modified magnetic nanoparticles functionalized with cetylpyridinium bromide for the preconcentration of metals after complexation with 8-hydroxyquinoline, *Talanta* 84 (2011) 83–89, <https://doi.org/10.1016/j.talanta.2011.02.013>.
- [18] P. Montoro-Leal, J.C. García-Mesa, M.M. López Guerrero, E. Vereda Alonso, Comparative study of synthesis methods to prepare new functionalized adsorbent materials based on MNPs-GO coupling, *Nanomaterials* 10 (2020) 304–322, <https://doi.org/10.3390/nano10020304>.
- [19] M.M. López Guerrero, E. Vereda Alonso, J.M. Cano Pavón, M.T. Siles Cordero, A. García de Torres, Simultaneous determination of chemical vapour generation forming elements (As, Bi, Sb, Se, Sn, Cd, Pt, Pd, Hg) and non-chemical vapour forming elements (Cu, Cr, Mn, Zn, Co) by ICP-OES, *J. Anal. At. Spectrom.* 31 (2016) 975–984, <https://doi.org/10.1039/C5JA00471C>.
- [20] P. Montoro-Leal, J.C. García-Mesa, M.M. López Guerrero, E. Vereda Alonso, *Material compuesto adsorbente de metales basado en óxido de grafeno magnético y procedimiento de obtención*, P202030050, 2021.
- [21] J. Rouquerol, D. Avnir, C.W. Fairbridge, D.H. Everett, J.M. Haynes, N. Pernicone, Recommendations for the characterization of porous solids (Technical Report), *Pure Appl. Chem.* 66 (1994) 1739–1758, <https://doi.org/10.1351/pac199466081739>.
- [22] M.C. Bruzzoniti, O. Abollino, M. Pazzi, L. Rivoira, A. Giacomino, M. Vincenti, Chromium, nickel, and cobalt in cosmetic matrices: an integrated bioanalytical characterization through total content, bioaccessibility, and Cr(III)/Cr(VI) speciation, *Anal. Bioanal. Chem.* 409 (2017) 6831–6841, <https://doi.org/10.1007/s00216-017-0644-8>.
- [23] A. Gáspár, J. Posta, R. Tóth, On-line chromatographic separation and determination of chromium(III) and chromium(VI) with preconcentration of the chromium(III) using potassium hydrogen phthalate, in various samples by flame atomic absorption spectrometry, *J. Anal. At. Spectrom.* 11 (1996) 1067–1074, <https://doi.org/10.1039/JA9961101067>.
- [24] J. Namiésnik, A. Rabajczyk, Speciation analysis of chromium in environmental samples, *Crit. Rev. Environ. Sci. Technol.* 42 (2012) 327–377, <https://doi.org/10.1080/10643389.2010.518517>.
- [25] F. Zewdu, M. Amare, Determination of the level of hexavalent, trivalent, and total chromium in the discharged effluent of Bahir Dar tannery using ICP-OES and UV-Visible spectrometry, *Cogent Chem* 4 (2018) 1534566–1534576, <https://doi.org/10.1080/23312009.2018.1534566>.
- [26] M.C. Yebra, R.M. Cespón, Determination of hexavalent chromium in welding fumes by flow injection flame atomic absorption spectrometry after dynamic alkaline ultrasound-assisted extraction/anion exchange preconcentration, *At. Spectrosc.* 29 (2008) 27–31.
- [27] J.L. Feng, C.F. Li, Chromium speciation and its stable isotopic signature in the dolomite-terra rossa weathering system, *Geoderma* 339 (2019) 106–114, <https://doi.org/10.1016/j.geoderma.2018.12.047>.
- [28] A. Aparna, M. Sumithra, G. Venkateswarlu, A.C. Sahayam, S.C. Chaurasia, T. Mukherjee, Speciation of Cr(III) and Cr(VI) in Seawater after Separation with a Sulphate-form of DOWEX-1 and ETAAS Determination Atomic Spectroscopy vol. 27, 2006, pp. 123–127.
- [29] T. Sumida, T. Ikenoue, K. Hamada, A. Sabarudin, M. Oshima, S. Motomizu, On-line preconcentration using dual mini-columns for the speciation of chromium(III) and chromium(VI) and its application to water samples as studied by inductively coupled plasma-atomic emission spectrometry, *Talanta* 68 (2005) 388–393, <https://doi.org/10.1016/j.talanta.2005.08.064>.
- [30] C.R.T. Tarley, G.F. Lima, D.R. Nascimento, A.R.S. Assis, E.S. Ribeiro, K.M. Diniz, Novel on-line sequential preconcentration system of Cr(III) and Cr(VI) hyphenated with flame atomic absorption spectrometry exploiting sorbents based on chemically modified silica, *Talanta* 100 (2012) 71–79, <https://doi.org/10.1016/j.talanta.2012.08.023>.
- [31] P. Liang, T. Shi, H. Lu, Z. Jiang, B. Hu, Speciation of Cr(III) and Cr(VI) by nanometer titanium dioxide micro-column and inductively coupled plasma atomic emission spectrometry, *Spectrochim. Acta Part B At. Spectrosc.* 58 (2003) 1709–1714, [https://doi.org/10.1016/S0584-8547\(03\)00136-8](https://doi.org/10.1016/S0584-8547(03)00136-8).
- [32] M.A. Chamjangali, N. Goudarzi, M. Mirheidari, B. Bahramian, Sequential eluent injection technique as a new approach for the on-line enrichment and speciation of Cr(III) and Cr(VI) species on a single column with FAAS detection, *J. Hazard Mater.* 192 (2011) 813–821, <https://doi.org/10.1016/j.jhazmat.2011.05.095>.
- [33] K. Saygi, M. Tuzen, M. Soylak, L. Elci, Chromium speciation by solid phase extraction on Dowex M 4195 chelating resin and determination by atomic absorption spectrometry, *J. Hazard Mater.* 153 (2008) 1009–1114, <https://doi.org/10.1016/j.jhazmat.2007.09.051>.
- [34] A. Tunçeli, Speciation of Cr(III) and Cr(VI) in Water after Preconcentration of its 1,5-diphenylcarbazone Complex on Amberlite XAD-16 Resin and Determination by FAAS, *Talanta* 57, 2002, [https://doi.org/10.1016/S0039-9140\(02\)00237-0](https://doi.org/10.1016/S0039-9140(02)00237-0), 1199–204.
- [35] M.Z. Corazza, E.S. Ribeiro, M.G. Segatelli, C.R.T. Tarley, Study of cross-linked poly (methacrylic acid) and polyvinylimidazole as selective adsorbents for on-line preconcentration and redox speciation of chromium with flame atomic absorption spectrometry determination, *Microchem. J.* 117 (2014) 18–26, <https://doi.org/10.1016/j.microc.2014.05.016>.
- [36] V.N. Alves, N.M.M. Coelho, Selective extraction and preconcentration of chromium using Moringa oleifera husks as biosorbent and flame atomic absorption spectrometry, *Microchem. J.* 109 (2013) 16–22, <https://doi.org/10.1016/j.microc.2012.05.030>.
- [37] K.M. Diniz, C.R.T. Tarley, Speciation analysis of chromium in water samples through sequential combination of dispersive magnetic solid phase extraction using mesoporous amino-functionalized Fe₃O₄/SiO₂ nanoparticles and cloud point extraction, *Microchem. J.* 123 (2015) 185–195, <https://doi.org/10.1016/j.microc.2015.06.011>.
- [38] A. Islam, H. Ahmad, N. Zaidi, S. Kumar, A graphene oxide decorated with triethylenetetramine-modified magnetite for separation of chromium species prior to their sequential speciation and determination via FAAS, *Microchim. Acta* 183 (2016) 289–296, <https://doi.org/10.1007/s00604-015-1641-2>.
- [39] C. Jinshun, G. Weixi, Z. Yuheng, Z. Xiashi, Fe₃O₄-SiO₂-graphene oxide-amino acid ionic liquid magnetic solid-phase extraction combined with inductively coupled plasma optical emission spectrometry for speciation of Cr(III) and Cr(VI) in environmental water, *New J. Chem.* 46 (2022) 3178–3184.
- [40] I. Narin, M. Soylak, K. Kayakirilmaz, L. Elci, M. Dogan, Speciation of Cr(III) and Cr(VI) in tannery wastewater and sediment samples on ambersorb 563 resin., *Anal. Lett.*, 35 8, 1437-1452. <https://doi.org/10.1081/AL-120006679>.
- [41] V. Numan Bulut, D. Ozdes, O. Bekircan, A. Gundogdu, C. Duran, M. Soylak, Carrier element-free coprecipitation (CEFC) method for the separation, preconcentration and speciation of chromium using an isatin derivative, *Anal. Chim. Acta* 632 (2009) 35–41.